The EMBO Journal vol.9 no.12 pp.4127-4133, 1990

Translational repression by a complex between the iron-responsive element of ferritin mRNA and its specific cytoplasmic binding protein is position-dependent *in vivo*

Britta Goossen, S.Wright Caughman[1], Joe B.Harford[2], Richard D.Klausner[2] and Matthias W.Hentze

European Molecular Biology Laboratory, Meyerhofstrasse 1, Postfach 102209, D-6900 Heidelberg 1, FRG, [1]Dermatology Branch, National Cancer Institute, and [2]Cell Biology and Metabolism Branch, National Institute of Child Health and Human Development, National Institutes of Health, Bethesda, MD 20892, USA

Communicated by I.W.Mattaj

The interaction of ferritin mRNA is regulated by iron via the interaction of a cytoplasmic binding protein (IRE-BP) with a specific stem-loop structure in the 5′ untranslated region (UTR), referred to as the iron-responsive element (IRE). A high affinity RNA-protein complex between the IRE and the IRE-BP functions as a repressor of translation *in vivo*. Translational repression appears to depend upon the position of the IRE in the 5′ UTR of the mRNA. IREs located in the 5′ untranslated region 67 nucleotides or more downstream of the 5′ terminus of the mRNA fail to mediate iron-dependent translational regulation and give rise to constitutively derepressed transcripts. A model is proposed in which translational regulation of protein biosynthesis involves a position-dependent interference of the IRE/IRE-BP complex with one of the initial steps in translation initiation.

Key words: gene expression / iron-responsive element/ ribosome/RNA-protein interactions/translation

Introduction

Translational control is a physiologically important mechanism of gene regulation in eukaryotic cells. Examples of translationally regulated systems include the mRNA for the transcription factor GCN4 (Miller and Hinnebusch, 1989; Tzamaris *et al.*, 1989), heat shock mRNAs (McGarry and Lindquist, 1985; Hultmark *et al.*, 1986), viral RNAs (Sonenberg, 1987; Pelletier and Sonenberg, 1988), developmentally regulated mRNAs (Strickland *et al.*, 1988; McGrew *et al.*, 1989), and the mRNAs which encode the iron storage protein ferritin (Zahringer *et al.*, 1976). In all of these examples, the process of translation initiation is the target of regulation.

In contrast to prokaryotes, where the ribosomes bind to an internal region of the mRNA close to the initiator AUG codon (Maitra *et al.*, 1982), eukaryotic mRNAs usually make first contact with the small ribosomal subunit (as part of the 43S pre-initiation complex) at or near the 5′ end of the transcript (Moldave, 1985; Kozak, 1989a). It is well known that the presence of a cap structure (^{7}mGpppX) at the 5′ terminus of eukaryotic mRNAs enhances the rate of binding of the 43S pre-initiation complex to the mRNA (Banerjee, 1980; Shatkin, 1985). The cap itself serves as a binding site for the cap-binding complex [CBC] (elF-4F, CBP II) which consists of several polypeptides. Binding of CBC to the cap is followed by unwinding of RNA secondary structure, a process which is mediated by the RNA helicase activity of elF-4A (Ray *et al.*, 1985; Sarkar *et al.*, 1985) and which appears to facilitate the interaction between the mRNA and the 43S pre-initiation complex (Abramson *et al.*, 1987). This initial binding step has been proposed to be followed by a scanning process of the 43S complex in a 5′ to 3′ direction (Kozak, 1989a). The complex migrates until it arrests at the initiator AUG codon (Kozak, 1986). At the initiator codon, the 60S subunit will join the 43S complex to form an 80S ribosome and translation begins.

Previous studies examined the effect of mRNA secondary structure on translation initiation by insertional mutagenesis (Pelletier and Sonenberg, 1985a; Kozak, 1986, 1988, 1989b). It was shown that the introduction of stem-loop structures positioned near the cap site inhibits translation. When such structures are placed further downstream, but within the 5′ UTR, inhibition of translation requires more stable structures, with a calculated Gibbs energy in the range of −50 kcal/mol (Kozak, 1986). Furthermore, an experimentally introduced stem-loop structure resulted in the loss of the ability to cross-link an 80 kd protein corresponding to the elF-4B which can normally be cross-linked to the cap structure after irradiation with ultraviolet light when the inserted stem-loop was close to the 5′ end of the transcript (Pelletier and Sonenberg, 1985b). These observations and others (for reviews see Sonenberg, 1988, and Kozak, 1989a) allow two major conclusions: (i) secondary structure within the 5′ UTR can influence the efficiency of translation initiation; and, (ii) the effect of secondary structure is not uniform throughout the 5′ UTR, but depends on its position with respect to the cap site.

The translation of ferritin mRNA provides a highly conserved, physiologically regulated model system which permits experimental access to several questions pertaining to general principles of translation in eukaryotic cells. All full-length ferritin cDNAs cloned thus far contain a characteristic, moderately stable stem-loop structure with a loop sequence of 5′ CAGTGN 3′ in the 5′ UTR (Hentze *et al.*, 1988). This element has been shown to be necessary and sufficient for iron-dependent translational regulation of ferritin mRNAs and has therefore been termed 'iron-responsive element' or 'IRE' (Aziz and Munro, 1987; Hentze *et al.*, 1987a,b). The IRE serves as the binding site for a specific cytoplasmic binding protein of ~90 kd which is referred to as 'IRE-binding protein' or 'IRE-BP' (Leibold and Munro, 1988; Rouault *et al.*, 1988). The iron status of the cell correlates with alterations in the affinity with which the IRE-BP can bind to the IRE (Haile *et al.*, 1989; Hentze *et al.*, 1989a). Under conditions of iron deprivation, when the rate of translation of ferritin mRNA is low, the number of high affinity IRE-BPs found in the cytosol increases. Con-

versely, when iron is plentiful, conditions under which ferritin mRNA translation is high, little if any high affinity IRE-BP activity is found in the cytosol. These results suggested that the high affinity binding of the IRE-BP to its target RNA correlated with the repression of translation. Direct support for this came from *in vitro* studies where the addition of partially purified IRE-BP to a cell-free translation system, derived from a wheat germ extract, results in the specific inhibition of ferritin biosynthesis (Walden *et al.*, 1988). Finally, we have demonstrated that the presence of the IRE stem–loop structure in the 5′ UTR of an mRNA correlates with the inhibition of translatability (Caughman *et al.*, 1988). This inhibition is relieved in the presence of iron, again suggesting that the IRE-BP, via its interaction with the IRE, acted *in vivo* as a translational repressor. A limitation to such an interpretation of this last study was the fact that the difference in translatability correlated with a gross difference in the structure of the 5′ UTR in terms of the presence or the absence of the IRE stem–loop. To investigate the role of the high affinity interaction of the IRE-BP with the IRE in translational control more accurately, we have taken advantage of the observation that the 5′ C residue of the IRE loop is critical for its function (Hentze *et al.*, 1988; Rouault *et al.*, 1988; Casey *et al.*, 1989). We have designed indicator constructs which permit variation in the number and/or position of IREs within the 5′ UTR without affecting the predicted secondary structure of the 5′ UTRs or the nucleotide sequences which surround the IREs. We here confirm that the IRE/IRE-BP complex functions as a translational repressor *in vivo*. However, we demonstrate that the ability of the IRE to serve as a *cis*-acting translational regulatory element is strictly dependent upon its position with respect to the cap structure of the transcript. Thus, IRE/IRE-BP complex formation within the 5′ UTR alone is not sufficient for translational repression.

Results

The IRE mediates translational repression in vivo

The observations outlined above suggest that binding of the IRE-BP to the IRE represses rather than enhances the ability of ferritin mRNA to be translated. More direct support for such a model should compare the translation efficiencies ('translatability') of mRNAs which differ only with regard to the presence or absence of a functional IRE, but which have the same potential for secondary structure formation and near identical nucleotide sequences. To address this question, we designed synthetic oligodeoxyribonucleotides which were cloned eight nucleotides downstream from the transcription start site and 62 nucleotides upstream of the AUG initiator codon of a previously described human growth hormone (hGH) indicator construct (Hentze *et al.*, 1987b; Casey *et al.*, 1988). These oligodeoxyribonucleotides contain four potential IRE motifs which are separated by a spacer consisting of six adenosine residues (Figure 1). The sequences of the two halves of the so-called 'lower stem' (Hentze *et al.*, 1988) of each potential IRE were chosen to ensure that they would base-pair only with the complementary sequence from the same IRE and not with one of the other three IRE motifs. In addition, this design permitted the introduction of restriction sites which were utilized in subsequent experiments (see below). The constructs were designed to contain either 'functional' IREs (six-membered loop sequence = CAGUGC) or 'non-functional' IREs (five-membered loop sequence = AGUGC). Of the four different IRE motifs in each construct, ones from which the critical 5′ C residue of the IRE loop has been omitted are indicated with a Δ. For example, in construct 1 + Δ3 × IRE-GH, the 5′ most IRE is structurally intact, whereas the remaining three motifs contain the single nucleotide deletion (Figure 1).

Initially, we compared the iron-responsiveness and

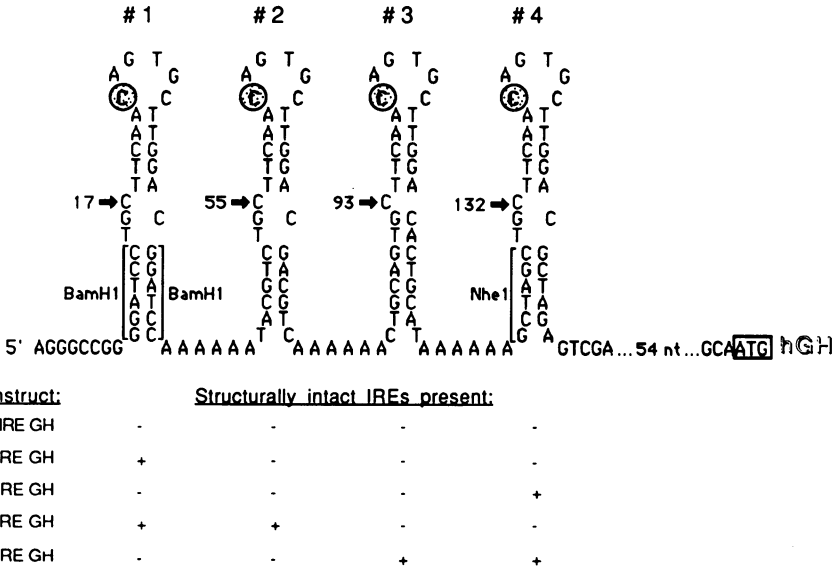

Fig. 1. Schematic representation of the 5′ untranslated region (UTR) of the human growth hormone (hGH) indicator constructs. The 5′ end of the nucleotide sequence corresponds to the transcription start site, the boxed ATG indicates the translation start site. No additional ATG triplets are located within the 5′ UTR. The 'C' residues which are marked with an arrow serve as reference points for the distance from the 5′ end of the transcript. The circled 'C' residues have been shown to be critical for IRE function and were utilized for variation of the structural integrity of a particular IRE, as shown in the bottom half of the figure. Restriction sites which were utilized in some constructs (Figure 4) are indicated by brackets.

translatabilities of two closely related indicator constructs which have been stably transfected into murine B6 cells. To alter the cellular iron status, transfectants were treated with hemin as a source of iron or the iron chelator desferrioxamine. The cells were then metabolically labeled with [^{35}S]methionine, and quantitative immunoprecipitation of hGH and endogenous murine ferritin was performed; in parallel, RNA was prepared from identically treated stable cell lines and analyzed by Northern blotting with an hGH specific DNA probe. The two constructs differed only by the presence (1 + Δ3 × IRE-GH) or absence (Δ4 × IRE-GH) of a single C residue in the loop of IRE # 1 and thus contained either one or no structurally intact IRE. If the IRE was the binding site for a translational repressor, the translatability (unit of hGH biosynthesis per unit of hGH mRNA) of Δ4 × IRE-GH mRNA should be constitutively high when compared with its iron-responsive counterpart, at least under conditions of iron starvation.

The data shown in Figure 2 demonstrate that the IRE-BP indeed acts as a translational repressor *in vivo*. The hGH mRNA levels remain largely unaffected by hemin and desferrioxamine treatment (the lower signal in the lane from hemin treated 1 + Δ3 × IRE-GH cells is due to a difference in gel loading) and are essentially the same in the two cell lines; however, the iron-independent translation of Δ4 × IRE-GH mRNA is as high as the level of iron induction of the 1 + Δ3 × IRE-GH mRNA. The failure of Δ4 × IRE-GH mRNA to respond to iron manipulations is clearly due to the absence of a functional IRE from the indicator transcript, because the translation of endogenous murine ferritin mRNA is regulated identically in the two cell lines (Figure 2). The range of iron regulation (the H/D ratio) for 1 + Δ3 × IRE-GH closely resembles the H/D ratio of endogenous ferritin biosynthesis; this finding supports our previous conclusion (Caughman *et al.*, 1988) that the IRE is the only *cis*-acting element which is responsible for iron-regulated ferritin mRNA translation.

Position-dependent function of the IRE

Based on the results presented in Figure 2, we investigated the mechanism by which the RNA−protein complex inhibits translation. Since translation initiation is an asymmetric process which begins at the 5′ end of the mRNA and involves several steps before protein synthesis initiates at the AUG codon, the position of the IRE within the 5′ UTR might affect its ability to interfere with this multi-step process. It had previously been shown that the distance between the IRE and the initiator AUG could be manipulated over a range of 137 nucleotides without an effect on the ability of the IRE to function as a translational regulator (Hentze *et al.*, 1987b).

We hypothesized that the position of the IRE with regard to the 5′ cap structure might be functionally relevant. To investigate this question, we took advantage of the previously described constructs and generated three additional plasmids which contained either one or two structurally intact IREs. The invariant unpaired C residues at the 5′ end of the 'upper stem' of the IRE motif (marked by arrows in Figure 1) were used as reference points for the distance of a particular IRE from the 5′ end of the mRNA.

Figure 3 shows that a structurally intact IRE fails to regulate mRNA translation when present at position 132 (in construct Δ3 + 1 × IRE-GH) rather than position 17 (in construct 1 + Δ3 × IRE-GH). An IRE at position 93 (in construct Δ2 + 2 × IRE-GH) also does not exhibit IRE function. As predicted from the previous results (Figure 2), construct 2 + Δ2 × IRE-GH did display iron regulation. Interestingly, this mRNA with two structurally intact IREs has a similar H/D ratio as 1 + Δ3 × IRE-GH mRNA which contains only one IRE. Moreover, the dose−response patterns of the two transcripts to different concentrations of either hemin or desferrioxamine display no significant differences (unpublished observations). These findings indicate that the presence of an additional IRE in position 55 has no significant influence on the function of the more 5′ IRE. Consistent with this view, we have found that a construct which contains four IREs (in positions 17, 55, 93 and 132) is regulated similarly to the single IRE construct 1 + Δ3 × IRE-GH (position 17, data not shown).

Our interpretation that Δ3 + 1 × IRE-GH mRNA fails to regulate translation because the only structurally intact IRE (IRE # 4) is located far downstream from the cap site predicts that IRE motif # 4 should confer iron-dependent mRNA translation when moved closer to the cap site. We utilized the *Bam*HI restriction sites in our constructs for deletion of IRE motif # 1 (see Figure 1) from either

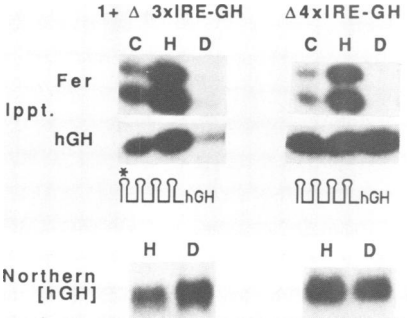

Fig. 2. The IRE binds a translational repressor *in vivo*. Stable transformants were analyzed by quantitative immunoprecipitation (Ippt.) after treatment with 100 μM hemin (H) or 100 μM desferrioxamine (D) and metabolic labeling with [^{35}S]methionine, or by Northern blotting with a human growth hormone (hGH) specific probe after identical treatment of the cells. In the upper panel, specifically precipitated hGH and endogenous murine ferritin H- and L-chains (Fer) are shown. Control samples which received neither hemin nor desferrioxamine are marked with a 'C'. The position of the structurally intact IRE is marked with an asterisk.

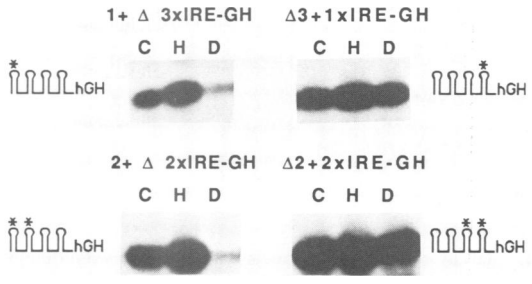

Fig. 3. Position-dependent function of the IRE. Stable transformants were analyzed by immunoprecipitation of metabolically labeled human growth hormone as described in Figure 2. Iron regulation of endogenous murine ferritins was similar in all four cell lines (not shown). The positions of structurally intact IREs are marked by an asterisk.

Δ3 + 1 × IRE-GH or Δ2 + 2 × IRE-GH to create Δ3 + 1 × IRE-GH[δ # 1] or Δ2 + 2 × IRE-GH[δ # 1]. In addition, we treated Δ3 + 1 × IRE-GH with *Bam*HI and *Nhe*I (Figure 1) to create Δ3 + 1 × IRE-GH[δ # 1,2,3]. The resulting deletion constructs were tested for iron regulation after transient expression in B6 fibroblasts.

It is evident from Figure 4 that the deletion construct Δ3 + 1 × IRE-GH[δ # 1,2,3] displays the same pattern of iron regulation as construct 1 + Δ3 × IRE-GH, which was included as a positive control. Thus, the IRE motif #4 is capable of conferring iron regulation when positioned sufficiently close to the 5′ end of the mRNA. The *Bam*HI deletions which remove the 5′ most IRE motif (26 nucleotides) from Δ3 + 1 × IRE-GH or Δ2 + 2 × IRE-GH both generate constructs which do not respond to iron perturbations. The failure of Δ3 + 1 × IRE-GH[δ # 1] to display iron regulation was expected, because the [δ # 1] deletion moved the structurally intact IRE motif #4 to position 106; the failure of Δ2 + 2 × IRE-GH[δ # 1] to be translationally regulated indicates that, at least in the context of these particular indicator constructs, even position 67 is too far 3′ from the cap structure to permit IRE function.

IRE/IRE-BP complex formation in the 5′ UTR is not sufficient for translational repression

Based on previous analyses of IRE structure and IRE-BP binding requirements (Hentze *et al.*, 1989a; Rouault *et al.*, 1988; Casey *et al.*, 1989; Haile *et al.*, 1989), we expected that the IRE-BP would be able to bind to the IRE motif #4 in the 5′ UTR of Δ3 + 1 × IRE-GH. In order to test this assumption, *Bgl*I restriction fragments which include the entire 5′ UTRs of the IRE-less construct Δ4 × IRE-GH, of the iron-responsive construct 1 + Δ3 × IRE-GH, and of the non-regulated construct Δ3 + 1 × IRE-GH were cloned into pGEM 3zf(−). *In vitro* transcripts were tested for their ability to form a ^{32}P-labeled IRE/IRE-BP complex or to compete for complex formation as unlabeled transcripts in mobility shift assays (Leibold and Munro, 1988). Figure 5 demonstrates that the *in vitro* transcripts derived from 1 + Δ3 × IRE-GH and Δ3 + 1 × IRE-GH can both bind the IRE-BP, whereas the Δ4 × IRE-GH transcript cannot engage in a high affinity interaction with the IRE-BP. The affinity constants for the transcripts derived from 1 + Δ3 × IRE-GH and Δ3 + 1 × IRE-GH were not directly measured. However, both transcripts appear to form IRE/IRE-BP complexes with equal efficiencies, and the IRE motif #4 binds the IRE-BP with sufficiently high affinity to mediate the iron regulation observed for construct Δ3 + 1 × IRE-GH[δ # 1,2,3] (Figure 4). A transcript corresponding to the regulatory region from the 3′ UTR of the human transferrin receptor [TfR] mRNA which has previously been shown to contain five IREs and to be responsible for iron-dependent regulation of TfR mRNA stability (Casey *et al.*, 1988; Mullner and Kuhn, 1988; Casey *et al.*, 1989), is shown as a positive control for IRE-BP binding. When added as unlabeled competitors in 500-fold molar excess, transcripts derived from the TfR (lanes a), 1 + Δ3 × IRE-GH (lanes b), and Δ3 + 1 × IRE-GH (lanes c) completely abolish complex formation with the ^{32}P-labeled probes. Transcripts from Δ4 × IRE-GH display partial competition (lanes d), presumably through a lower affinity interaction with the IRE-BP (Rouault *et al.*, 1988).

The results demonstrate that the 5′ UTR of

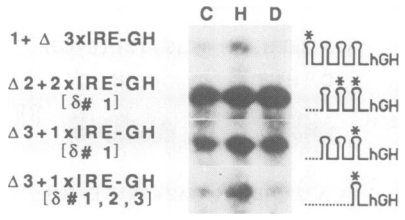

Fig. 4. Analysis of selected constructs with deletions within the 5′ UTR of the indicator constructs depicted in Figure 1. The indicated plasmid constructs were transiently expressed in murine B6 fibroblasts and analyzed for iron regulation by immunoprecipitation of human growth hormone as described in Figure 2. The range of iron regulation of mRNAs under translational control of functional IREs is known to show some experimental variation (Caughman *et al.*, 1988) and was in this experiment lower than in the experiments shown in Figures 2 and 3. The positions of structurally intact IREs are marked by an asterisk, dotted lines indicate regions of the 5′ UTR which were deleted from the parent constructs.

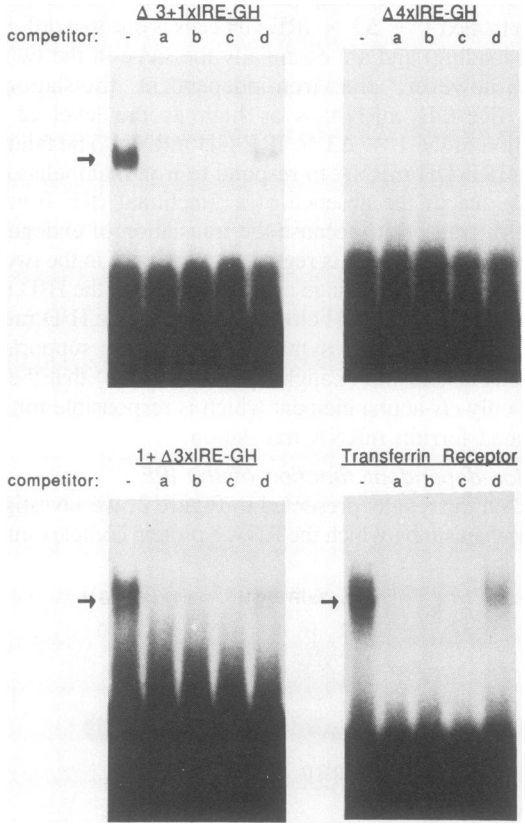

Fig. 5. Binding of the IRE-binding protein (IRE-BP) to iron-responsive elements *in vitro*. Restriction fragments including the complete 5′ untranslated regions of three indicator constructs or the iron regulatory region from the human transferrin receptor (TfR) cDNA (Casey *et al.*, 1988) were subcloned into pGEM vectors. [^{32}P]-labeled or unlabeled synthetic RNA was transcribed *in vitro* and analyzed by mobility shift assays for its ability to bind the murine IRE-BP. The transcript Δ4 × IRE-GH cannot engage in a high affinity interaction with the IRE-BP and shows no radiolabeled IRE/IRE-BP complex. However, high molar excess of unlabeled Δ4 × IRE-GH can partially compete for complex formation (Rouault *et al.*, 1988), presumably through a lower affinity interaction with the IRE-BP. The following competitors were used: TfR (**a**), 1 + Δ3 × IRE-GH (**b**), Δ3 + 1 × IRE-GH (**c**), andΔ4 × IRE-GH (**d**). The area of the specific IRE/IRE-BP complex is marked by an arrow.

Δ3 + 1 × IRE-GH can bind the IRE-BP *in vitro* and support our view that Δ3 + 1 × IRE-GH mRNA is translationally derepressed in spite of the ability of the mRNA to form a high affinity IRE/IRE-BP complex. These data suggest that the IRE/IRE-BP complex can only repress translation initiation when it is located sufficiently close to the cap site of the mRNA.

Discussion

We have employed transient and stable expression analyses to characterize the *in vivo* role of the IRE-binding protein and its binding site in the 5′ UTR of ferritin mRNA, the IRE. Our data demonstrate that the RNA−protein complex represses translation initiation and that this repression is dependent on the position of the IRE/IRE-BP complex with regard to the 5′ end of the mRNA.

All of our studies employ indicator constructs of similar design. We have attempted to compose the 5′ UTRs of the indicator constructs in a way which allows prediction of their secondary structures and which permits variation in the number and/or position of IREs with minimal consequent changes to the secondary structure of the 5′ UTR and the nucleotide context of the IREs. This particular design was chosen to eliminate, as far as possible, ambiguities in the interpretation which could result from non-specific effects of secondary structure and nucleotide composition on the efficiency of translation initiation. It should be noted that despite the presence of four IRE-like motifs, the overall degree of secondary structure formation apparently does not affect the initiation apparatus, since the translation efficiencies of mRNAs from the IRE-less construct Δ4 × IRE-GH and a related construct from which all four IRE-like motifs have been removed (deletion of nucleotides 13−147) are essentially identical (unpublished observations).

The data presented in Figures 3 and 4 suggest that a distance of 67 nucleotides or more between the cap structure and the IRE does not permit an IRE/IRE-BP complex to interfere with the process of translation initiation effectively. This distance assignment may depend to a certain extent on the tertiary structure of a particular mRNA. We are now attempting to define determinants of this 'distance threshold' in more detail. To this end, we have inserted a stuffer RNA element with little potential for secondary structure formation and without any IRE-like features between the transcription start site and the functional IRE of a previously analyzed iron-regulated indicator construct (referred to as TfR element C; Casey *et al.*, 1988). This insertion moves this transferrin receptor mRNA-derived IRE from position 20 to position 67 and renders it unresponsive to iron perturbations (unpublished observations). Thus, the position-dependence which we observe with the constructs used in this study was confirmed when different stuffer RNA elements were used to alter the distance of a functional IRE from the transcription start site. It is interesting that the distance between the IRE and the cap structure of six ferritin mRNAs from different species has been well conserved and ranges from 33 to 39 nucleotides (Theil, 1990). However, the sequence for a *Xenopus laevis* ferritin mRNA has recently been published and it contains an IRE sequence 174 nucleotides downstream of the cap site (Moskaitis *et al.*, 1990). Although it has not been directly demonstrated that this IRE is functional, if it proves to mediate translational regulation, we will need to reconcile the implications of this *Xenopus* sequence with the findings reported here.

Insertion mutagenesis has helped to demonstrate that secondary structure formation can influence the translational efficiency of a particular mRNA (Pelletier and Sonenberg, 1985a; Kozak, 1986) and that the effect of secondary structure may be more pronounced when the inserted motifs

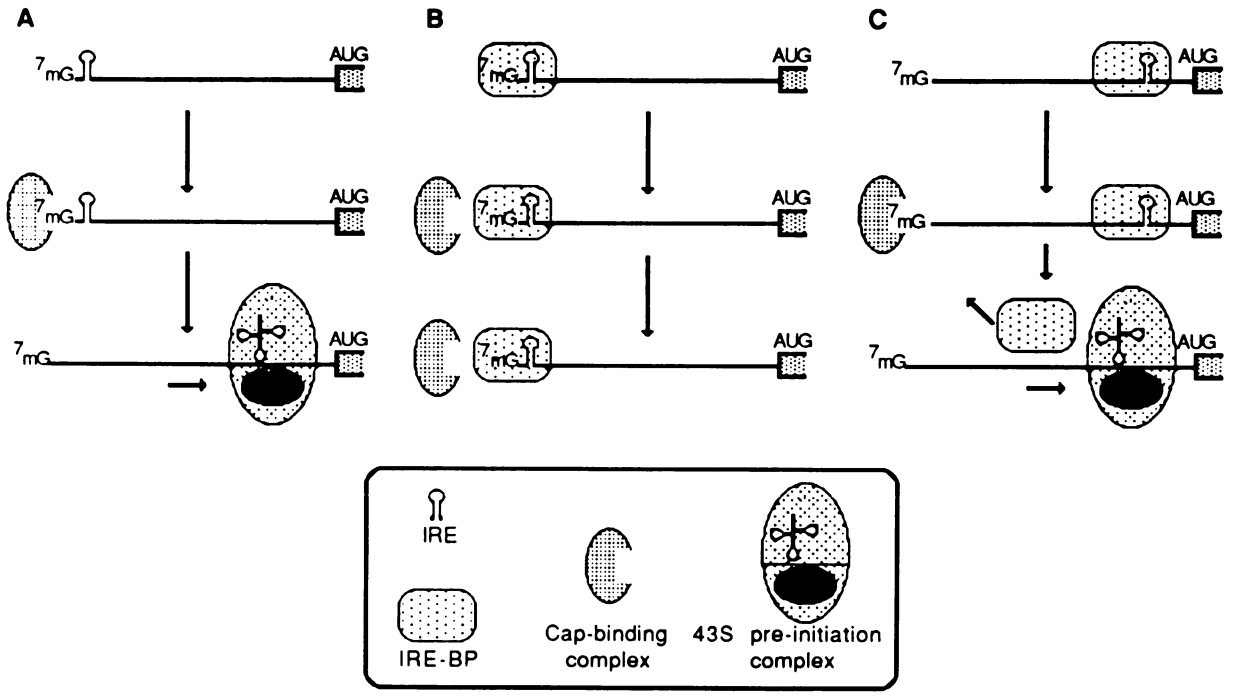

Fig. 6. A model for the position-dependent function of the IRE/IRE-BP complex as a translational repressor. Panel **A** depicts lack of IRE-binding of the IRE-BP in iron-replete cells, panels **B** and **C** show high affinity IRE/IRE-BP complexes in iron starved cells. For a more detailed discussion, see text.

are placed in close proximity to the cap site (Pelletier and Sonenberg, 1985b; Kozak, 1989b). Such studies clearly demonstrate that the process of translation initiation can be subject to inhibitory influences by *cis*-acting sequences within the 5′ UTR. For a translationally regulated system which requires more than 100-fold changes in translational efficiency, one might envisage a strong inhibitory stem−loop motif which would be specifically recognized by a 'melting protein'. Alternatively, a relatively weak stem−loop which by itself would not impede translation initiation may serve as a binding site for a regulated translational repressor protein. The function of the protein could either be to stop binding of the CBC by steric hindrance, to interfere with translation initiation by stabilization of the hairpin−loop structure, or by active enzymatic modulation of CBC function. The ferritin IRE/IRE-BP complex appears to be the first physiological eukaryotic example for such a regulatory system.

Analyses of position−function relationships have had significant impact on our understanding of several genetic regulatory mechanisms. Examples include transcriptional regulatory elements like the TATA box and enhancers (Hochschild and Ptashne, 1986; Dynan, 1989), signals for transcription termination and polyadenylation (Birnstiel *et al.*, 1985; Platt, 1986), and splicing signals (Keller, 1984). The next challenge which the IRE/IRE-BP system poses will be to define the molecular mechanisms by which the RNA−protein complex represses translation. While several models for this repression are possible, any model proposed should accommodate the position requirement for IRE/IRE-BP function. Figure 6 depicts such a model. Under conditions of cellular iron load (Figure 6A), the IRE-BP does not bind to the IRE (Klausner and Harford, 1989) and the 'free' IRE does not impede translation initiation mediated by binding of the cap-binding complex [CBC] and subsequent interaction of the 43S pre-initiation complex with the ferritin mRNA. Under conditions of cellular iron starvation (Figure 6B), the IRE-BP would form a complex with the IRE, which in turn would impede either binding of the CBC or subsequent functionally critical steps. Our current data do not distinguish between a blockage to CBC binding or inhibition of subsequent events. In a strict sense, our model would not even require that the IRE/IRE-BP complex interferes with the CBC. We are currently investigating whether the IRE requires cap-dependent translation initiation for function or whether it can also regulate cap-independent translation initiation on a polio-virus derived template (Pelletier and Sonenberg, 1988). In either case, the IRE/IRE-BP complex fails to repress translation in iron-starved cells when the complex is located too far downstream from the 5′ end of the mRNA (Figure 6C). This model would be consistent with both the 'scanning model' as proposed by Kozak (1989a) and the 'melting model' suggested by Sonenberg (1988).

The IRE-BP has been shown to be capable of binding to the IRE *in vitro* with picomolar affinity (Haile *et al.*, 1989). While this binding affinity may be different *in vivo*, it is remarkable that such a potentially stable RNA−protein complex can apparently be overcome efficiently during translation initiation if it is located far enough downstream from the 5′ end of the mRNA. This report provides the first evidence that specific mRNA−protein complexes can be dissociated or bypassed during translation initiation. Our findings also establish a functionally critical spatial coupling between two mRNA elements, the 5′ terminus and the IRE, which play a role in translation initiation. If nature has taken advantage of a similar strategy for translational regulation in other systems, our findings would suggest that the responsible *cis*-acting elements may generally be found in close proximity to the transcription start site.

Materials and methods

Plasmid constructions

All indicator constructs used in this report are derived from the previously described L5-GH plasmid (Casey *et al.*, 1988) which contains adjacent 5′ *Bam*HI and *Xba*I 3′ sites sandwiched between the well characterized transcription start site of the ferritin promoter (Costanzo *et al.*, 1986; Hentze *et al.*, 1986) and the protein coding region of the human growth hormone gene. Pairs of complementary oligodeoxyribonucleotides (corresponding to nucleotides 10−151 in Figure 1) were synthesized with an Applied Biosystems DNA synthesizer and purified on a 10% polyacrylamide gel. They were annealed, phosphorylated, and the double stranded DNA was cloned between the *Bam*HI and *Xba*I sites of L5-GH. The correct nucleotide sequences of the insertions of the resultant plasmids were confirmed by DNA sequencing as previously described (Casey *et al.*, 1988). The sequence for construct Δ4 × IRE-GH was: 5′GGATCCTGCTTCAAAGTGCTTGGA CGGATCCAAAAAATACGTCTGCTTCAAAGTGCTTGGACGACGT CAAAAAACTGCAGTGCTTCAAAGTGCTTGGACACTGCATAAAA AAGCTAGCTGCTTCAAAGTGCTTGGACGCTAGA 3′. As indicated in Figure 1, similar oligodeoxyribonucleotides with insertions of a 'C' residue at appropriate positions (5′ of the underlined 'A' residues above) were also prepared, cloned and analyzed in the same way to generate 1 + Δ3 × IRE-GH, Δ3 + 1 × IRE-GH, 2 + Δ2 × IRE-GH, and Δ2 + 2 × IRE-GH.

For the construction of Δ3 + 1 × IRE-GH[δ # 1] and Δ2 + 2 × IRE-GH[δ # 1], the parent plasmids Δ3 + 1 × IRE-GH and Δ2 + 2 × IRE-GH were digested to completion with *Bam*HI which removed IRE motif # 1. The large fragments were gel purified, religated and cloned. For the construction of Δ3 + 1 × IRE-GH[δ # 1,2,3], the parent plasmid Δ3 + 1 × IRE-GH was digested to completion with *Bam*HI and *Nhe*I, the larger fragment was gel purified, protruding 5′ ends were filled in with the Klenow fragment of DNA polymerase, religated, and cloned. The deletions of the intended nucleotides were confirmed in all cases by high resolution restriction mapping.

The *in vitro* transcription vectors utilized in Figure 5 were constructed as follows: the parent plasmids 1 + Δ3 × IRE-GH, Δ3 + 1 × IRE-GH, and Δ4 × IRE-GH were digested to completion with *Bgl*I, and 1.7 kb restriction fragments including the regions which correspond to the entire 5′ UTR were gel purified, blunt-ended with T4 DNA polymerase, and cloned into the *Sma*I site of pGEM-3zf(−) (Promega, Madison, Wisconsin, USA). The integrity of the regions corresponding to the 5′ UTR were reconfirmed by DNA sequencing. The plasmid labeled 'TfR' was generated by purification of a 0.678 kb restriction fragment corresponding to nucleotides 3178 to 3856 of the human transferrin receptor cDNA (Schneider *et al.*, 1984), blunt-ended with the Klenow fragment of DNA polymerase, and cloned into the *Sma*I site of pGEM-3zf(−).

Cell culture and transfections

Stable transformants were generated as previously described (Hentze *et al.*, 1986) by cotransfection of the hGH indicator plasmid with the herpes simplex virus thymidine kinase gene into murine B6 fibroblasts and subsequent selection in medium containing hypoxanthine, aminopterin, and thymidine (HAT). All stable cell lines were maintained in HAT medium. Transient expression experiments were performed by the calcium phosphate precipitation method as described (Hentze *et al.*, 1987a).

Analysis of ^{35}S-labeled proteins

Transiently transfected or stably transformed cells were incubated at 37°C for 4 h with 100 μM hemin or 100 μM desferrioxamine, washed twice with methionine-free medium, and labeled with 40 μCi/ml [^{35}S]methionine for 2 h at 37°C. Quantatitive immunoprecipitation with polyclonal anti-ferritin antibodies, or polyclonal anti-hGH antibodies (National Hormone and Pituitary Program, Baltimore, MD, USA), analysis by SDS−PAGE, and autoradiography were performed as described (Caughman *et al.*, 1988).

Mobility shift assays

Detergent extracts were prepared from murine B6 fibroblasts which had been stably transfected with an unrelated plasmid and which were maintained in HAT medium as previously described (Hentze *et al.*, 1989b). ^{32}P-labeled

or unlabeled *in vitro* transcripts were generated as described (Hentze *et al.*, 1989b). Briefly, the recombinant pGEM plasmids were linearized with the appropriate restriction enzymes and transcribed with either SP6 RNA polymerase or T7 RNA polymerase to yield uncapped synthetic transcripts which resemble the sense orientation of the corresponding mRNA. Equal aliquots (10 μg) of detergent extract were incubated with 100 000 c.p.m. of the appropriate probe (specific activity $\sim 1 \times 10^8$ c.p.m./μg RNA) at 22°C; where indicated, a 500-fold molar excess of unlabeled competitor RNA was added to the extract 2 min prior to the addition of probe. After 30 min, 1.0 U RNase T1 was added for 10 min, and 3 mg/ml heparin were added subsequently for an additional 10 min. Analysis of RNA–protein complexes by non-denaturing gel electrophoresis and autoradiography was performed as previously described (Leibold and Munro, 1988).

Northern blotting

Total cellular RNA was prepared from 3×10^7 stably transfected cells which were treated with hemin and desferrioxamine as described above. Cells were solubilized in guanidinium isothiocyanate and RNA was recovered after ultracentrifugation through a CsCl cushion. Equal aliquots (10 μg) of RNA were subjected to electrophoresis through 0.7% agarose gels in the presence of formaldehyde, and to electrotransfer onto nylon membranes. Equal loading of the different lanes was assessed by inspection of ribosomal RNAs of the ethidium bromide stained gels. The nylon membranes were analyzed by hybridization with a ^{32}P-labeled probe which corresponds to a 600 nucleotide *Sma*I fragment from the human growth hormone gene.

Acknowledgements

The authors are especially thankful to Drs Bernhard Dobberstein, Angus Lamond, Iain Mattaj, David Tollervey, and to Professor Lennart Philipson for carefully reading the manuscript and for making helpful suggestions. We thank the National Hormone and Pituitary Program (University of Maryland School of Medicine) and the National Institute of Diabetes and Digestive and Kidney Diseases for the gift of polyclonal antisera against human growth hormone.

References

Abramson,R.D., Dever,T.E., Lawson,T.G., Ray,B.K., Thach,R.E. and Merrick,W.C. (1987) *J. Biol. Chem.*, **262**, 3826–3832.
Aziz,N. and Munro,H.N. (1987) *Proc. Natl. Acad. Sci. USA*, **84**, 8478–8482.
Banerjee,A.K. (1980) *Microbiol. Rev.*, **44**, 175–205.
Birnstiel,M.L., Busslinger,M. and Strub,K. (1985) *Cell*, **41**, 349–359.
Casey,J.L., Hentze,M.W., Koeller,D.M., Caughman,S.W., Rouault,T.A., Klausner,R.D. and Harford,J.B. (1988) *Science*, **240**, 924–928.
Casey,J.L., Koeller,D.M., Ramin,V.C., Klausner,R.D. and Harford,J.B. (1989) *EMBO J.*, **8**, 3693–3699.
Caughman,S.W., Hentze,M.W., Rouault,T.A., Harford,J.B. and Klausner,R.D. (1988) *J. Biol. Chem.*, **263**, 19048–19052.
Costanzo,F., Colombo,M., Staempfli,S., Santoro,C., Marone,M., Frank,R., Delius,H. and Cortese,R. (1986) *Nucleic Acids Res.*, **14**, 721–736.
Dynan,W.S. (1989) *Cell*, **58**, 1–4.
Haile,D.J., Hentze,M.W., Rouault,T.A., Harford,J.B. and Klausner,R.D. (1989) *Mol. Cell. Biol.*, **9**, 5055–5061.
Hentze,M.W., Keim,S., Papadopoulos,P., O'Brien,S., Modi,W., Drysdale,J., Leonard,W.L., Harford,J.B. and Klausner,R.D. (1986) *Proc. Natl. Acad. Sci. USA*, **83**, 7226–7230.
Hentze,M.W., Rouault,T.A., Caughman,S.W., Dancis,A., Harford,J.B. and Klausner,R.D. (1987a) *Proc. Natl. Acad. Sci. USA*, **84**, 6730–6734.
Hentze,M.W., Caughman,S.W., Rouault,T.A., Barriocanal,J.G., Dancis,A., Harford,J.B. and Klausner,R.D. (1987b) *Science*, **238**, 1570–1573.,
Hentze,M.W., Caughman,S.W., Casey,J.L., Koeller,D.M., Rouault,T.A. Harford,J.B. and Klausner,R.D. (1988) *Gene*, **72**, 201–208.
Hentze,M.W., Rouault,T.A., Harford,J.B. and Klausner,R.D. (1989a) *Science*, **244**, 357–359.
Hentze,M.W., Seuanez,H.N., O'Brien,S.J., Harford,J.B. and Klausner,R.D. (1989b) *Nucleic Acids Res.*, **17**, 6103–6108.
Hochschild,A. and Ptashne,M. (1986) *Cell*, **44**, 681–687.
Hultmark,D., Klemenz,R. and Gehring,W.J. (1986) *Cell*, **44**, 429–438.
Keller,W. (1984) *Cell*, **39**, 423–425.
Klausner,R.D. and Harford,J.B. (1989) *Science*, **246**, 870–872.
Kozak,M. (1986) *Proc. Natl. Acad. Sci. USA*, **83**, 2850–2854.
Kozak,M. (1988) *Mol. Cell. Biol.*, **8**, 2737–2744.
Kozak,M. (1989a) *J. Cell Biol.*, **108**, 229–241.
Kozak,M. (1989b) *Mol. Cell. Biol.*, **9**, 5134–5142.
Leibold,E.A. and Munro,H.N. (1988) *Proc. Natl. Acad. Sci. USA*, **85**, 2171–2175.
Maitra,U., Stringer,E.A. and Chaudhuri,A. (1982) *Annu. Rev. Biochem.*, **51**, 869–900.
McGarry,T.J. and Lindquist,S. (1985) *Cell*, **42**, 903–911.
McGrew,L.L., Dworkin-Rastl,E., Dworkin,M.B. and Richter,J.D. (1989) *Genes Dev.*, **3**, 803–815.
Miller,P.F. and Hinnebusch,A.G. (1989) *Genes Dev.*, **3**, 1217–1225.
Moldave,K. (1985) *Annu. Rev. Biochem.*, **54**, 1109–1149.
Moskaitis,J.E., Pastori,R.L. and Schoenberg,D.R. (1990) *Nucleic Acids Res.*, **18**, 2184.
Mullner,E.W. and Kuhn,L.C. (1988) *Cell*, **53**, 815–825.
Mullner,E.W., Neupert,B. and Kuhn,L.C. (1989) *Cell*, **58**, 373–382.
Pelletier,J. and Sonenberg,N. (1985a) *Cell*, **40**, 515–526.
Pelletier,J. and Sonenberg,N. (1985b) *Mol. Cell. Biol.*, **5**, 3222–3230.
Pelletier,J. and Sonenberg,N. (1988) *Nature*, **334**, 320–325.
Platt,T. (1986) *Annu. Rev. Biochem.*, **55**, 339–372.
Ray,B.K., Lawson,T.G., Kramer,J.C., Cladaras,M.H., Grifo,J.A., Abramson,R.D., Merrick,W.C. and Thach,R.E. (1985) *J. Biol. Chem.*, **260**, 7651–7658.
Rouault,T.A., Hentze,M.W., Caughman,S.W., Harford,J.B. and Klausner,R.D. (1988) *Science*, **241**, 1207–1210.
Sarkar,G., Edery,I. and Sonenberg,N. (1985) *J. Biol Chem.*, **260**, 13831–13837.
Schneider,C., Owen,M.J., Banville,D. and Williams,J.G. (1984) *Nature*, **311**, 675–678.
Shatkin,A.J. (1985) *Cell*, **40**, 223–224.
Sonenberg,N. (1987) *Adv. Virus Res.*, **33**, 175–204.
Sonenberg,N. (1988) *Prog. Nucleic Acids Res. Mol. Biol.*, **35**, 173–207.
Strickland,S., Huarte,J., Belin,D., Vassalli,A., Rickles,R.J. and Vassalli,J.-D. (1988) *Science*, **241**, 680–684.
Theil,E.C. (1990) *J. Biol. Chem.*, **265**, 4771–4774.
Tzamaris,D., Roussou,I. and Thireos,G. (1989) *Cell*, **57**, 947–954.
Walden,W.E., Daniels-McQueen,S., Brown,P.H., Gaffield,L., Russel,D.A., Bielser,D., Bailey,L.C. and Thach,R.E. (1988) *Proc. Natl. Acad. Sci. USA*, **85**, 9503–9507.
Zahringer,J., Baliga,B.S. and Munro,H.N. (1976) *Proc. Natl. Acad. Sci. USA*, **73**, 857–861.

Received on August 9, 1990; revised on August 23, 1990